Synsint Research Group

Available online at www.synsint.com

Synthesis and Sintering

ISSN 2564-0186 (Print), ISSN 2564-0194 (Online)

Review article

Non-catalytic applications of g-C_3N_4: A brief review

Milad Sakkaki *, Seyed Mohammad Arab

Department of Mechanical Engineering, University of Mohaghegh Ardabili, P.O. Box 179, Ardabil, Iran

ABSTRACT

The g-C_3N_4 which is well known as a polymeric non-metal semiconductor, has been fabricated by thermal polymerization. It has also been used in catalytic applications including, photo-catalysis, removal and degradation of pollutants in water, Friedel-Crafts reactions, oxygen reduction reaction and etc. It has drawn noticeable research attention due to its economical and affordable fabrication, non-toxicity, biocompatibility, good thermal and electrical conductivity, high hardness, Corrosion resistance, and fireproofing properties. Therefore, the g-C_3N_4 has found non-catalytic applications including composites, cutting tools, improving surface properties, light emitting devices, optical sensors, and solar cells. In the current review, the novel and non-catalytic applications of g-C_3N_4 have been highlighted.

KEYWORDS

Graphitic carbon nitride (g-C_3N_4)
Cutting tools
Composite
Non-catalytic applications

OPEN ACCESS

1. Introduction

Among different C_3N_4 carbon nitride allotropes i.e., the g-C_3N_4, α-C_3N_4, β-C_3N_4, cubic C_3N_4, and pseudo-cubic C_3N_4, the g-C_3N_4 (graphitic carbon nitride) which is classified as a polymeric material, is the most stable specie under the ambient condition [1–4]. Blasius et al. have investigated a material that was named "melon" (linear polymers of connected tri-s-triazines via secondary nitrogen) and had been reported by Liebig [5–8]. They could be synthesized by substituting carbon atoms with nitrogen in carbon materials**.** Heating up followed by a single-step polymerization of cheap organic feedstock such as dicyandiamide, cyanamide, urea, thiourea, and melamine which is containing C and N, with earth-abundant elements have been used for preparing Graphitic carbon nitrides [6–10]. Unlike conventional organic semiconductors, g-C_3N_4 exhibits unique thermal and chemical stability [11, 12]. Due to other special properties of g-C_3N_4 such as non-toxicity, medium band gap, economical productivity, and environmental compatibility, different studies on g-C_3N_4 have been highly regarded [13–16]. The g-C_3N_4 has been used as a catalyst for different applications such as water treatment [17], Friedel-Crafts reactions [18, 19], and oxygen reduction reactions [20, 21]. Wastewater treatment and recycling is one of the most challenging problems in the world, particularly the wastewater produced by chemical industries, because of its remarkable concentration of large organic fragments which are tremendously poisonous and carcinogenic [22, 23]. Polymeric materials have been widely employed in water treatment applications. Graphitic carbon nitride, a two-dimensional organic polymeric material is also used as an effective adsorbent and photocatalyst for the fast removal and degradation of various pollutants in wastewater [24].

Recently, the g-C_3N_4 has been used in non-catalytic applications for example as a photoelectronic material. It has been used also as a sintering aid and reinforcement agent in manufacturing ultra-high temperature composites (UHTCs) fabricated by spark plasma sintering (SPS). The SPS is a new method used to fabricate the parts through powder technology [25]. The SPS uses the axial pressure and electrical current concurrently based on the Joule heating phenomenon to bond the powder particles. The Joule heat source and the material properties such as thermal conductivity, electrical resistivity, specific heat, and density are important parameters in the SPS process. Spark plasma sintering has been used to fabricate which are difficult to fabricate by more common methods such as casting. Ultra-high-temperature ceramics have been generally fabricated by the SPS process [26–28]. UHTCs have attracted many of attention due to their desirable mechanical properties, thermal and chemical stability at high temperatures, very high hardness, and corrosion resistance [29, 30].

* Corresponding author. *E-mail address:* sakkakimilad@student.uma.ac.ir, sakkakimilad@gmail.com (M. Sakkaki)
Received 24 October 2022; Received in revised form 29 December 2022; Accepted 30 December 2022.
Peer review under responsibility of Synsint Research Group.
https://doi.org/10.53063/synsint.2022.24126

Using the SPS process in the manufacture of UHTCs will be very useful [31]. The SPS process has faced some challenges in cases in which powder has low sinter-ability, poor oxidation resistance, and low self-diffusion coefficient [32]. Some research has been carried out to solve the mentioned problems in order to improve the properties of parts manufactured with the SPS process by adding the g-C_3N_4 as a sintering aid and reinforcement phase. This review study has highlighted novel and non-catalytic applications of g-C_3N_4 (Fig. 1).

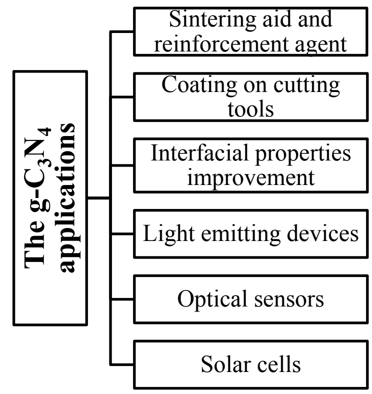

Fig. 1. Non-catalytic applications of g-C_3N_4.

2. Applications

2.1. Sintering aid and reinforcement phase in composites

Ahmadi et al. [9] have used the g-C_3N_4 as a sintering aid and reinforcement phase in the ZrB_2 Matrix fabricated through the SPS process. They have attempted to solve the sintering problems of ZrB_2 and improve the properties. They have reported that by the addition of 5 wt% of g-C_3N_4 to ZrB_2-based composite, the sinter-ability significantly improved. The relative density in g-C_3N_4 doped ZrB_2 ceramics in comparison with monolithic ZrB_2 is reduced from 76.5% to an approximately fully dense ceramic (to about 99.8%).

According to Fig. 2a, porosities are observed in the sintered sample in absence of C_3N_4 which showed incomplete sintering. By adding C_3N_4 to the ZrB_2 matrix, the in-situ synthesis of new phases has taken place in the C_3N_4-ZrB_2 composite which has been propagated in the pore-free ZrB_2 matrix (Fig. 2b).

The XRD analysis indicated that adding 5 wt% C_3N_4 to ZrB_2, has revealed some new peaks in the ZrB_2 XRD pattern. Generally, the ZrB_2, C_3N_4, ZrC, and BN peaks were identified. The oxide impurities also have been detected in the sintered sample after the SPS processing. The new phases could have been formed according to the following reactions [9].

$$C_3N_4 = 3C + 2N_2(g) \quad (1)$$

$$ZrB_2 + C + N_2(g) = ZrC + 2BN \quad (2)$$

$$ZrO_2 + 3C = ZrC + 2CO(g) \quad (3)$$

$$B_2O_3 + 3C + N_2(g) = 2BN + 3CO(g) \quad (4)$$

The mechanical properties also have been improved by adding 5 wt% C_3N_4 to the ZrB_2 matrix, due to densification enhancement and grain growth reduction. The Vickers hardness, fracture toughness, and flexural strength have been increased from 10.1 GPa, 1.9 $MPam^{½}$, and 187.6 MPa to 16.2 GPa, 5.4 $MPam^{½}$, and 516.4 MPa, respectively [33].

2.2. Coating on cutting tools

The C_3N_4 is a very hard and resistant to wear component which has a low coefficient of friction, and acceptable thermal conductivity [34, 35]. Therefore using the C_3N_4 as a coating for cutting tools seems a very attractive idea. Yang et al. [36] have applied a C_3N_4 film on the CN-coated YT15 cutter. They have used a lathe machine to examine the performance of CN-coated YT15 cutting tools on a cylinder sample made of hardened 45 steel. The machining condition has been as follows:

- Dry cutting (without liquid)
- Tool work angles: $\gamma_o = 15°$, $\alpha_o = 10°$, $K_r = 45°$, and $r_\varepsilon = 0.12$ mm
- Machining parameters: V_c = 40-90 m/min, ap = 0.1–0.4 mm, and f = 0.03–0.12 mm/r.

The tool flank wear-time curve is shown in Fig. 3. The tool life has been increased remarkably with the C_3N_4 coating compared to the uncoated one. The film also has enhanced the tool's thermal resistance which has made it an appropriate choice for dry-cutting processes.

Three types of wear have been investigated, i.e. flank, rake, and crater wear. The main forms have been the rake and flank wear. The rake wear has been the dominant one during high-speed cutting with a higher cutting depth. The worn surface of the tool is shown in Fig. 4.

2.3. Agent to improve the interfacial properties of carbon fiber

The application of graphitic carbon nitride in polymer matrix composites is developing a stronger interface between carbon fiber and epoxy [37–40]. The stronger adhesion between the matrix and the reinforcement leads to better mechanical properties, otherwise, the volume occupied by the secondary phase in the matrix will act as a discontinuity which will weaken the properties [41].

Song et al. [40] have increased the roughness and wetting ability of carbon fiber through an in situ precipitation of C_3N_4 on carbon fiber. The nitride changed the surface morphology of carbon fiber (Fig. 5). The addition of C_3N_4, in fact, increased the roughness of the carbon

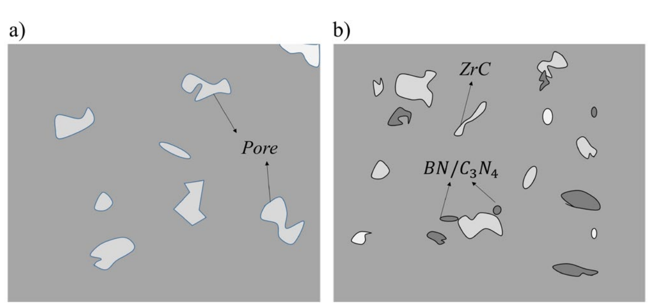

Fig. 2. The schematic representation of the polished surfaces of a) ZrB_2 and b) C_3N_4-doped ZrB_2 ceramics [9].

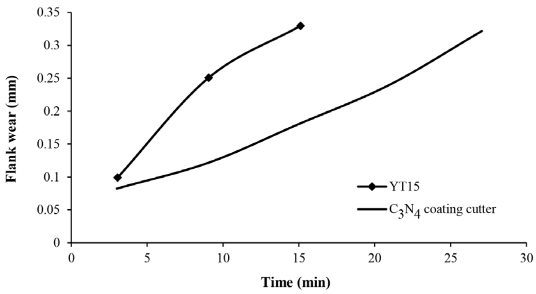

Fig. 3. The tool flank wear-time curve under the condition: V_c = 60 m/min, f = 0.1 mm/r, and ap = 0.4 mm [36].

fibers. The inter-laminar shear strength (ILSS) and interfacial shear strength (IFSS) of composites reinforced with the fibers have been increased from 44.3 and 43.1 MPa to 60.7 and 75.9 MPa, respectively. Moreover, the surface free energy of carbon fibers has been increased by 65.6%. The improved interfacial properties have resulted in a higher tensile strength (from 1063 to 1279 MPa) and total absorbed energy of impact examination (from 1.22 to 1.75 J). The dynamic mechanical properties and hydrothermal aging resistance have been enhanced significantly. In addition, the storage modulus has been enhanced from 64.3 to 74.1 GPa.

The presence of nitrogen improves the properties of carbonaceous materials including mechanical properties, structural, and in particular electrical properties. The sp^2 hybridization between nitrogen and carbon forms a π-conjugated electronic structure which endows it with excellent photoelectronic properties [6]. Nowadays, due to the particular electrical properties of C_3N_4, it has found special applications in solar cells, fuel cells, light-emitting devices, and batteries.

2.4. Light-emitting device

Recently, due to the semi-conductivity of g-C_3N_4, numerous investigations have been concentrated on the luminescence properties of g-C_3N_4 [42, 43]. Some studies have been performed to explain the mechanism of visible photoluminescence (PL) of carbon nitride. The photoluminescence area is dominated by the optical band gap and it was indicated that the band gap of g-C_3N_4 is tunable with processing temperature [44, 45]. Zhang et al. [46] have studied the photoluminescence tune-ability of synthesized g-C_3N_4 nanopowder. The powder has been fabricated by low-temperature thermal condensation of melamine. They observed phase transformation from melamine to amorphous g-C_3N_4 by increasing the processing temperature. They reported that the morphology altered from a granular to a layer structure with different dimensions of flakes. The resulting emission area of the samples envelops from 400 nm to 510 nm, varying from blue-violet to green by continuously controlling the processing temperature.

Because of the biocompatibility and non-toxicity of C_3N_4, its application instead of noxious substances in LEDs has drawn considerable attention. Conventional LEDs contain hazardous components such as PbS, CdTe, CuInS, CdSe, and CdS, which raise toxicity and pollution problems. The advantages of white-light-emitting diodes (WLEDs) compared to conventional LEDs, are including high efficiency, low power consumption, extended lifetime, and fast response which has introduced the WLEDs as a suitable alternative to conventional LEDs.

Wang et al. [47] have used the g-C_3N_4 silica-gels to develop WLEDs with non-metal and biocompatible materials. They have synthesized pure g-C_3N_4 nanoparticles by heating up a mixture of 0.4 g of anhydrous citric acid and 0.4 g thiourea in the air at 180 °C for 2 hours. The dip coating technique has been used to precipitate a g-C_3N_4 film on the glass of the LED lamp. The optimal wavelength of 365 nm also has been selected. The fabricated WLED had more flexibility, lower cost, higher quantum efficiency and color rendering index of 70, and also higher transparency.

2.5. The optical sensors

The need for accurate, sensitive, rapid, and simple detectors that have sufficient biocompatibility and reliability becomes more and more every day. Optical sensors are molecular receptors whose optical properties change upon binding to specific guests. One of the most important applications of these sensors is to detect metallic ions (chromogenic/fluorescent receptors) [5, 48]. Many studies have tried to reduce the limitations and enhance the kinetic response of sensors. The g-C_3N_4 could carry functional groups such as NH_2/NH/N on its surface to endow enormously absorption of metal ions via redox or chelation reactions. Regarding the current features of chromogenic/fluorescent receptors, the g-C_3N_4 is an attractive candidate for employment in optical sensors. The sensitivity of the g-C_3N_4 is higher than the sensors with optical receptors because optical receptors hooks on the porous medium while g-C_3N_4 acts as a receptor itself [48, 49].

2.6. Solar applications

The use of fossil fuels is facing challenges due to limited resources, pollution, environmental crises, and global warming. Thus, clean energy production from renewable and biocompatible sources especially solar energy become a very important issue. Among various types of solar cells including Bio-hybrid, Buried Contact, Cadmium Telluride, and Concentrated PV Cell, dye-sensitized solar cells (DSSC) are very interesting because of easy fabrication, low cost, and environmentally friendly properties [50]. The g-C_3N_4, as a tenuous band gap semiconductor and sufficient visible light-absorbing abilities, could be an additive to enhance solar cell performance [51]. Xu et al. [52] have fabricated TiO_2@g-C_3N_4 nano-sheets by heating the mixture of urea and TiO_2 nano-sheets employed as a photo-anode material of DSSCs. The g-C_3N_4 nanosheet is a π-conjugated material, which is a proper choice for separating the photogenerated electron-hole pairs. The g-C_3N_4 films could act as a blocking layer that efficiently prevents charge recombination at the TiO_2/electrolyte interface in DSSC. As a consequence, the thin layer of the g-C_3N_4 on the TiO_2 surface can effectively promote electron transportation by prorogating the backward recombination of electrons from TiO_2 and electrolyte and contributing additional electrons to boost the electron concentration in the photo-anodes. This leads to enhancing the performance of DSSC.

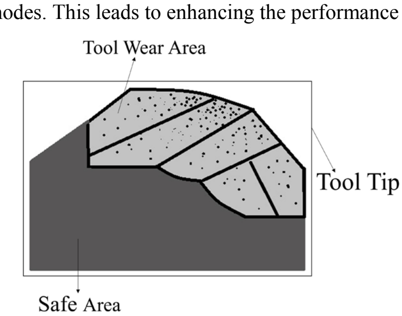

Fig. 4. The schematic image for rake wear in C_3N_4-coated cutter [36].

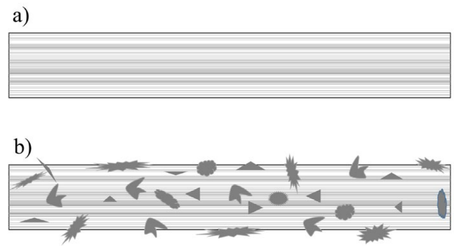

Fig. 5. The schematic micrograph of a) carbon fiber and b) carbon fiber coated by C_3N_4 [40].

3. Conclusions

Graphitic carbon nitride (g-C_3N_4) as an appealing member of materials with attractive properties has been used widely in different applications. The g-C_3N_4 had been mostly used in catalytic applications such as photocatalysis, removal, and degradation of water pollution, Friedel-Crafts reactions, and oxygen reduction reaction. Recently, it has been used in some non-catalytic applications due to its good thermal and chemical stability, proper mechanical properties, applicable energy band gap, non-toxicity, and cost-effectiveness. It has found special applications in materials engineering including composites reinforcement, sintering aid, coating of cutting tools, solar cells, light-emitting devices, and medical applications.

CRediT authorship contribution statement

Milad Sakkaki: Conceptualization, Investigation, Writing – original draft.

Seyed Mohammad Arab: Conceptualization, Investigation, Writing – review & editing.

Data availability

The data underlying this article will be shared on reasonable request to the corresponding author.

Declaration of competing interest

The authors declare no competing interests.

Funding and acknowledgment

This article is based on the master thesis of the first author. The authors are grateful to the University of Mohaghegh Ardabili for their financial support under grant number 1401-d-14-23513.

References

[1] Y.T. Yew, C.S. Lim, A.Y.S. Eng, J. Oh, S. Park, M. Pumera, Electrochemistry of Layered Graphitic Carbon Nitride Synthesised from Various Precursors: Searching for Catalytic Effects, ChemPhysChem. 17 (2016) 481–488. https://doi.org/10.1002/cphc.201501009.

[2] Y. Miyamoto, M.L. Cohen, S.G. Louie, Theoretical investigation of graphitic carbon nitride and possible tubule forms, Solid State Commun. 102 (1997) 605–608. https://doi.org/10.1016/S0038-1098(97)00025-2.

[3] A. Y. Liu R.M. Wentzcovitch, Stability of carbon nitride solids, Phys. Rev. B. 50 (1994) 10362–10365. https://doi.org/10.1103/PhysRevB.50.10362.

[4] A.Y. Liu, M.L. Cohen, Structural properties and electronic structure of low-compressibility materials, Phys. Rev. B. 41 (1990) 10727–10734. https://doi.org/10.1103/PhysRevB.41.10727.

[5] E.Z. Lee, Y.-S. Jun, W. H. Hong, A. Thomas, M.M. Jin, Cubic mesoporous graphitic carbon(IV) nitride: an all-in-one chemosensor for selective optical sensing of metal ions, Angew. Chem. Int. Ed. 49 (2010) 9706–9710. https://doi.org/10.1002/anie.201004975.

[6] J. Zhu, P. Xiao, H. Li, S.A.C. Carabineiro, Graphitic Carbon Nitride: Synthesis, Properties, and Applications in Catalysis, ACS Appl. Mater. Interfaces. 6 (2014) 16449–16465. https://doi.org/10.1021/am502925j.

[7] J. Liebig, Uber einige Stickstoff - Verbindungen, Ann. Pharm. 10 (1834) 1–47. https://doi.org/10.1002/jlac.18340100102.

[8] A.Y. Liu, M.L. Cohen, Prediction of New Low Compressibility Solids, Sci. 245 (1989) 841–842. https://doi.org/10.1126/science.245.4920.841.

[9] Z. Ahmadi, M. Zakeri, A. Habibi-Yangjeh, M. Shahedi Asl, A novel ZrB2–C3N4 composite with improved mechanical properties, Ceram. Int. 45 (2019) 21512–21519. https://doi.org/10.1016/j.ceramint.2019.07.144.

[10] M. Mousavi, A. Habibi-Yangjeh, Ternary g-C3N4/Fe3O4/Ag3VO4 nanocomposites: Novel magnetically separable visible-light-driven photocatalysts for efficiently degradation of dye pollutants, Mater. Chem. Phys. 163 (2015) 421–430. https://doi.org/10.1016/j.matchemphys.2015.07.061.

[11] J. Yang, X. Wu, X. Li, Y. Liu, L. Kong, et al., Synthesis and characterization of nitrogen-rich carbon nitride nanobelts by pyrolysis of melamine, Appl. Phys. A. 105 (2011) 161–166. https://doi.org/10.1007/s00339-011-6471-4.

[12] E.G. Gillan, Synthesis of Nitrogen-Rich Carbon Nitride Networks from an Energetic Molecular Azide Precursor, Chem. Mater. 12 (2000) 3906–3912. https://doi.org/10.1021/cm000570y.

[13] P. Suyana, P. Ganguly, B.N. Nair, S.C. Pillai, U.S. Hareesh, Structural and compositional tuning in g-C3N4 based systems for photocatalytic antibiotic degradation, Chem. Eng. J. Adv. 8 (2021) 100148. https://doi.org/10.1016/j.ceja.2021.100148.

[14] Q. Hao, G. Jia, W. Wei, A. Vinu, Y. Wang, et al., Graphitic carbon nitride with different dimensionalities for energy and environmental applications, Nano Res. 13 (2020) 18–37. https://doi.org/10.1007/s12274-019-2589-z.

[15] L. Shen, Z. Xing, J. Zou, Z. Li, X. Wu, et al., Black TiO2 nanobelts/g-C3N4 nanosheets Laminated Heterojunctions with Efficient Visible-Light-Driven Photocatalytic Performance, Sci. Rep. 7 (2017) 41978. https://doi.org/10.1038/srep41978.

[16] Y. Yuan, L. Zhang, J. Xing, M.I.B. Utama, X. Lu, et al., High-yield synthesis and optical properties of g-C3N4, Nanoscale. 7 (2015) 12343–12350. https://doi.org/10.1039/C5NR02905H.

[17] Y. Wang, X. Wang, M. Antonietti, Polymeric Graphitic Carbon Nitride as a Heterogeneous Organocatalyst: From Photochemistry to Multipurpose Catalysis to Sustainable Chemistry, Angew. Chem. Int. Ed. 51 (2012) 68–89. https://doi.org/10.1002/anie.201101182.

[18] Q. Yang, W. Wang, Y. Zhao, J. Zhu, Y. Zhu, L. Wang, Metal-free mesoporous carbon nitride catalyze the Friedel–Crafts reaction by activation of benzene, RSC Adv. 5 (2015) 54978–54984. https://doi.org/10.1039/C5RA08871B.

[19] F. Goettmann, A. Fischer, M. Antonietti, A. Thomas, Chemical Synthesis of Mesoporous Carbon Nitrides Using Hard Templates and Their Use as a Metal-Free Catalyst for Friedel–Crafts Reaction of Benzene, Angew. Chem. Int. Ed. 45 (2006) 4467–4471. https://doi.org/10.1002/anie.200600412.

[20] X. Li, P. Cui, W. Zhong, J. Li, X. Wang, et al., Graphitic carbon nitride supported single-atom catalysts for efficient oxygen evolution reaction, Chem. Commun. 52 (2016) 13233–13236. https://doi.org/10.1039/C6CC07049C.

[21] H.-S. Zhai, L. Cao, X.-H. Xia, Synthesis of graphitic carbon nitride through pyrolysis of melamine and its electrocatalysis for oxygen reduction reaction, Chin. Chem. Lett. 24 (2013) 103–106. https://doi.org/10.1016/j.cclet.2013.01.030.

[22] A. Azanaw, B. Birlie, B. Teshome, M. Jemberie, Textile effluent treatment methods and eco-friendly resolution of textile wastewater,

Case Stud. Chem. Environ. Eng. 6 (2022) 100230. https://doi.org/10.1016/j.cscee.2022.100230.

[23] F.S.A. Khan, N.M. Mubarak, Y.H. Tan, M. Khalid, R.R. Karri, et al., A comprehensive review on magnetic carbon nanotubes and carbon nanotube-based buckypaper for removal of heavy metals and dyes, J. Hazard Mater. 413 (2021) 125375. https://doi.org/10.1016/j.jhazmat.2021.125375.

[24] K. Rathinam, M.M. Nara, I.M.A. ElSherbiny, I. Ali, S. Panglisch, Application of g-C3N4-based Materials for the Efficient Removal and Degradation of Pollutants in Water and Wastewater Treatment, Nanomaterials and Nanocomposites for Environmental Remediation, Springer, Singapore. (2021) 95–119. https://doi.org/10.1007/978-981-16-3256-3_5.

[25] M. Sakkaki, F. Sadegh Moghanlou, M. Vajdi, M. Shahedi Asl, M. Mohammadi, M. Shokouhimehr, Numerical simulation of heat transfer during spark plasma sintering of zirconium diboride, Ceram. Int. 46 (2020) 4998–5007. https://doi.org/10.1016/j.ceramint.2019.10.240.

[26] S.M. Bagheri, M. Vajdi, F. Sadegh Moghanlou, M. Sakkaki, M. Mohammadi, et al., Numerical modeling of heat transfer during spark plasma sintering of titanium carbide, Ceram. Int. 46 (2020) 7615–7624. https://doi.org/10.1016/j.ceramint.2019.11.262.

[27] E. Ranjbarpour Niari, M. Vajdi, M. Sakkaki, S. Azizi, F. Sadegh Moghanlou, M. Shahedi Asl, Finite element simulation of disk-shaped HfB 2 ceramics during spark plasma sintering process, Int. J. Appl. Ceram. Technol. 19 (2022) 344–357. https://doi.org/10.1111/ijac.13886.

[28] F. Adibpur, S.A. Tayebifard, M. Zakeri, M. Shahedi Asl, Spark plasma sintering of quadruplet ZrB2–SiC–ZrC–Cf composites, Ceram. Int. 46 (2020) 156–164. https://doi.org/10.1016/j.ceramint.2019.08.243.

[29] M. Shahedi Asl, B. Nayebi, Z. Ahmadi, M.J. Zamharir, M. Shokouhimehr, Effects of carbon additives on the properties of ZrB2–based composites: A review, Ceram. Int. 44 (2018) 7334–7348. https://doi.org/10.1016/j.ceramint.2018.01.214.

[30] E. Ghasali, M. Shahedi Asl, Microstructural development during spark plasma sintering of ZrB2–SiC–Ti composite, Ceram. Int. 44 (2018) 18078–18083. https://doi.org/10.1016/j.ceramint.2018.07.011.

[31] S.R. Levine, E.J. Opila, M.C. Halbig, J.D. Kiser, M. Singh, J.A. Salem, Evaluation of ultra-high temperature ceramics foraeropropulsion use, J. Eur. Ceram. Soc. 22 (2002) 2757–2767. https://doi.org/10.1016/S0955-2219(02)00140-1.

[32] R.M. Rocha, F.F. Sene, M.O. Juliani, C.O. Davi, Effect of ZrB2 Particle Size on Pressureless Sintering of ZrB2 - ß-Sic Composites, J. Aerosp. Technol. Manag. 11 (2019) e2819. https://doi.org/10.5028/jatm.v11.1049.

[33] Z. Ahmadi, M. Zakeri, M. Farvizi, A. Habibi-Yangjeh, S. Asadzadeh-Khaneghah, M. Shahedi Asl, Synergistic influence of SiC and C3N4 reinforcements on the characteristics of ZrB2 -based composites, J. Asian Ceram. Soc. 9 (2021) 53–62. https://doi.org/10.1080/21870764.2020.1847425.

[34] L. Zhang, H. Qi, G. Li, D. Wang, T. Wang, et al., Significantly enhanced wear resistance of PEEK by simply filling with modified graphitic carbon nitride, Mater. Des. 129 (2017) 192–200. https://doi.org/10.1016/j.matdes.2017.05.041.

[35] V. Matějka, M. Leonardi, P. Praus, G. Straffelini, S. Gialanella, The Role of Graphitic Carbon Nitride in the Formulation of Copper-Free Friction Composites Designed for Automotive Brake Pads, Metals (Basel). 12 (2022) 123. https://doi.org/10.3390/met12010123.

[36] H.D. Yang, X.Q. Xia, Z.H. Qing, Trial on C3N4 Coating Cutter Hard-Dry Cutting on Hardened Steel, Appl. Mech. Mater. 33 (2010) 483-486. https://doi.org/10.4028/www.scientific.net/AMM.33.483.

[37] T. Wang, B. Song, L. Wang, A new filler for epoxy resin: study on the properties of graphite carbon nitride (g-C3N4) reinforced epoxy resin composites, Polymers (Basel). 12 (2020) 76. https://doi.org/10.3390/polym12010076.

[38] B. Song, T. Wang, L. Wang, H. Liu, X. Mai, et al., Interfacially reinforced carbon fiber/epoxy composite laminates via in-situ synthesized graphitic carbon nitride (g-C3N4), Compos. B: Eng. 158 (2019) 259–268. https://doi.org/10.1016/j.compositesb.2018.09.081.

[39] S. Xiong, Y. Zhao, Y. Wang, J. Song, X. Zhao, S. Li, Enhanced interfacial properties of carbon fiber/epoxy composites by coating carbon nanotubes onto carbon fiber surface by one-step dipping method, Appl. Surf. Sci. 546 (2021) 149135. https://doi.org/10.1016/j.apsusc.2021.149135.

[40] B. Song, T. Wang, H. Sun, H. Liu, X. Mai, et al., Graphitic carbon nitride (g-C3N4) interfacially strengthened carbon fiber epoxy composites, Compos. Sci. Technol. 167 (2018) 515–521. https://doi.org/10.1016/j.compscitech.2018.08.031.

[41] S.-Y. Fu, X.-Q. Feng, B. Lauke, Y.-W. Mai, Effects of particle size, particle/matrix interface adhesion and particle loading on mechanical properties of particulate–polymer composites, Compos. B: Eng. 39 (2008) 933–961. https://doi.org/10.1016/j.compositesb.2008.01.002.

[42] B.B. Wang, Q.J. Cheng, L.H. Wang, K. Zheng, K. Ostrikov, The effect of temperature on the mechanism of photoluminescence from plasma-nucleated, nitrogenated carbon nanotips, Carbon. 50 (2012) 3561–3571. https://doi.org/10.1016/j.carbon.2012.03.028.

[43] D. Papadimitriou, G. Roupakas, C.A. Dimitriadis, S. Logothetidis, Raman scattering and photoluminescence of nitrogenated amorphous carbon films, J. Appl. Phys. 92 (2002) 870–875. https://doi.org/10.1063/1.1488251.

[44] R. Tang, D. Gong, Y. Deng, S. Xiong, J. Zheng, et al., π-π stacking derived from graphene-like biochar/g-C3N4 with tunable band structure for photocatalytic antibiotics degradation via peroxymonosulfate activation, J. Hazard Mater. 423 (2022) 126944. https://doi.org/10.1016/j.jhazmat.2021.126944.

[45] D. Wang, X. Huang, Y. Huang, X. Yu, Y. Lei, et al., Self-assembly synthesis of petal-like Cl-doped g-C3N4 nanosheets with tunable band structure for enhanced photocatalytic activity, Colloids Surf. A: Physicochem. Eng. Asp. 611 (2021) 125780. https://doi.org/10.1016/j.colsurfa.2020.125780.

[46] Y. Zhang, Q. Pan, G. Chai, M. Liang, G. Dong, et al., Synthesis and luminescence mechanism of multicolor-emitting g-C3N4 nanopowders by low temperature thermal condensation of melamine, Sci. Rep. 3 (2013) 1943. https://doi.org/10.1038/srep01943.

[47] A. Wang, C. Lee, H. Bian, Z. Li, Y. Zhan, et al., Synthesis of g-C3N4 /Silica Gels for White-Light-Emitting Devices, Part. Part. Syst. Charact. 34 (2017) 1600258. https://doi.org/10.1002/ppsc.201600258.

[48] E.W. Stein, P.S. Grant, H. Zhu, M.J. McShane, Microscale Enzymatic Optical Biosensors Using Mass Transport Limiting Nanofilms. 1. Fabrication and Characterization Using Glucose as a Model Analyte, Anal. Chem. 79 (2007) 1339–1348. https://doi.org/10.1021/ac061414z.

[49] G. Dong, Y. Zhang, Q. Pan, J. Qiu, A fantastic graphitic carbon nitride (g-C3N4) material: Electronic structure, photocatalytic and photoelectronic properties, J. Photochem. Photobiol. C: Photochem. Rev. 20 (2014) 33–50. https://doi.org/10.1016/j.jphotochemrev.2014.04.002.

[50] M.B. Asgari, V. Mirzaei Mahmoud Abadi, M. Mirhabibi, Types of Solar Cells and Application, Am. J. Opt. Photonics. 3 (2015) 94. https://doi.org/10.11648/j.ajop.20150305.17.

[51] S. Asadzadeh-Khaneghah, A. Habibi-Yangjeh, M. Shahedi Asl, Z. Ahmadi, S. Ghosh, Synthesis of novel ternary g-C3N4/SiC/C-Dots photocatalysts and their visible-light-induced activities in removal of various contaminants, J. Photochem. Photobiol. A: Chem. 392 (2020) 112431. https://doi.org/10.1016/j.jphotochem.2020.112431.

[52] J. Xu, G. Wang, J. Fan, B. Liu, S. Cao, J. Yu, g-C3N4 modified TiO2 nanosheets with enhanced photoelectric conversion efficiency in dye-sensitized solar cells, J. Power Sources. 274 (2015) 77–84. https://doi.org/10.1016/j.jpowsour.2014.10.033.